IAC-22,A1,3,1,x68643

A compact pulsed near-infrared light probe for non-invasive imaging of the spaces between the skull and the brain to improve the diagnosis of brain injuries during spaceflight

Roxanne Fournier[a]*, Kwasi Nkansah[b], Myles G. Harris[c], Kaizad Raimalwala[d], Tovy Kamine[e], Timotheus Gmeiner[f]

[a] *Department of Chemical and Biological Engineering, University of British Columbia, 2360 E Mall, Vancouver, BC, Canada V6T 1Z3,* roxyfour@mail.ubc.ca
[b] *Department of Medicine, University of Toronto, 27 King's College Circle Toronto, ON M5S 1A1 kwasi.nkansah@mail.utoronto.ca*
[c] *Institute for Risk and Disaster Reduction, University College London, Gower St, London WC1E 6BT, United Kingdom,* myles.harris.19@ucl.ac.uk
[d] *Mission Control Space Services, 162 Elm St. West, Ottawa, ON K1R 6N5,* kaizad@missioncontrolspaceservices.com
[e] *UMass-Chan School of Medicine-Baystate, 55 N Lake Ave, Worcester, MA 01655, United States*, tovy.kamine@gmail.com
[f] *Buildwonder*, timo@buildwonder.co
* Corresponding Author

Abstract

An intracranial hemorrhage (IH) is a medical emergency that needs to be managed within hours of the event. In the context of deep space travel, this signifies that an emergency evacuation back to Earth, which could take many days, would not be possible. Additionally, the gold-standard for diagnosis of IH, computed tomography (CT), is resource intensive, generates ionizing radiation, and requires special training to operate and interpret. For these reasons, it is unlikely that CT scans will be available for astronauts in space for years to come. To address this problem, we have designed a novel diagnostic tool that will provide crew medical officers or their crewmates with information on the presence and severity of an IH by taking advantage of recent advancements in the field of time-domain diffuse correlation spectroscopy. The device consists of a pulsed laser generator and handheld probe which is able to emit light and gather reflected diffuse light that has travelled through the skull. As the laser will be pulsed as opposed to a continuous beam, it allows us to determine the time-of-flight (TOF) and lag time of the photons based on fluctuations in the intensity of light. Additionally, the ultrafast femtosecond pulse will gather information on the composition of the biological tissue being examined. The end result will be data on the depth and velocity of light scattering particles of the tissue to an approximate maximal depth of 2-3 cm, as well as the amplitude and phase of the collected light. Because IH changes the optical properties of the meningeal layers, we expect to be able to feed particle velocity data into a custom machine learning algorithm to learn to identify bleeds. The overall design does not exceed the volume of a double-width ISS middeck locker, making it compact enough to meet spaceflight requirements. The design also includes a framework that will enable the data to be quickly transmitted to healthcare providers off-site such as a flight surgeon on Earth managing a deep space mission. In addition to being able to detect changes in optical properties of meningeal layers, we also anticipate applications for diagnosis and management of pleural effusion In conclusion, by reducing the reliance on medevacs back to Earth in order to perform CT scans, and by providing more evidence in the hands of the user, we can increase the autonomy of astronaut crews in deep space.

Keywords: intracranial hemorrhage, astronaut healthcare, near-infrared spectroscopy, diffuse correlation spectroscopy, brain imaging

Nomenclature

β = intensity autocorrelation function contrast
g = field autocorrelation function
M = exponential term over which g is summated
t_s = photon time-of-flight
τ = photon lag time
$\xi_m(t_s)$ = TOF-dependent decay autocorrelation function

Acronyms/Abbreviations

Autocorrelation function (ACF), bovine serum albumin (BSA), cerebrospinal fluid (CSF), computed tomography (CT), confidence interval (CI) electroencephalogram (EEG), generative adversarial networks (GANs), Glasgow Coma Scale (GCS), international space station (ISS), intracranial hemorrhage (IH), magnetic resonance imaging (MRI), near-infrared (NIR), phosphate-buffered saline (PBS),

polydimethylsiloxane (PDMS), polyurethane (PU), red blood cell (RBC), relative blood flow index (rBFI), traumatic brain injury (TBI), terahertz (THz), time-of-flight (TOF), user interface (UI)

1. Introduction

Intracranial hemorrhages (IH) are serious, life-threatening conditions that necessitate rapid assessment by healthcare providers. IH are commonly caused by trauma; factors such as high blood pressure or weakened blood vessels are also predisposing factors. Following IH, blood from damaged blood vessels infiltrate the meningeal spaces, which can lead to increased intracranial pressure in part by increased fluid volume and by irritation of meningeal tissue by blood components [1]. Without expeditious diagnosis, monitoring, and treatment, an unresolved intracranial bleed can be fatal within as little as a few hours. Unfortunately, the signs and symptoms often go unnoticed until irreversible damage and death of brain tissue has occurred. The current gold standard diagnostic tool for detecting IH, non-contrast computed tomography (CT), is large, expensive, and requires special training to operate and interpret the resulting images. For these reasons, there is an immediate need for novel diagnostic tools that can be used effectively in a pre-hospital care setting, notably in remote areas that lack significant medical infrastructure. This applies to areas on Earth with unreliable phone connections, internet, reduced electricity, cumbersome transportation logistics. As an extension of this, spaceflight can be a considered a remote prehospital setting for which non-invasive monitoring and the diagnosis of intracranial hemorrhages is essential for creating a quick and effective management plan for preventing significant morbidity due to intracranial hemorrhages.

1.1 A primer on intracranial hemorrhages

1.1.1. Epidural Hematomas

The classical arterial epidural hematoma occurs following blunt trauma to the temporal region of the head. There is typically a skull fracture with damage to the middle meningeal artery causing arterial bleeding into the potential epidural space. They can account for approximately 2% of head injury patients and account for 5% to 15% of fatal head injuries [2]. The classic presentation is a loss of consciousness after the injury, followed by a lucid interval then neurologic deterioration. Expansion of the IH can lead to the Cushing response (hypertension, bradycardia, and bradypnea).

1.1.2. Subdural Hematomas

Commonly subdural hemorrhage occurs after a blunt injury causing damage between vessels traversing between the brain and skull; it results in bleeding in the subdural space. They account for an estimated 5% to 25% of patients with a significant head injury [2]. Findings on presentation may demonstrate a focal motor deficit, neurologic deficits, lethargy, or altered consciousness.

1.1.3. Subarachnoid hemorrhages

Typically, subarachnoid hemorrhages occur when the cortical surface vessels are injured and bleed into the subarachnoid space. They can be caused by trauma, as well as aneurysms, arteriovenous malformations, use of blood thinners, or idiopathic causes. The classic description for individuals suffering from these hemorrhages is a ‘thunderclap headache’ - a sudden severe headache or worst headache of life.

1.2 Current management of head trauma in space

Managing head trauma has proven difficult because the surface of the skull may appear closed and intact whilst serious pathology is brewing, resulting in serious and potentially irreversible morbidity. Diagnostic tools for visualizing beneath the skull such as CT or MRI machines tend to be expensive, require specialists, or limited in availability. As a consequence of this, countries have developed different validated decision making tools to triage patients with traumatic head injuries into different risk categories and provide an indication of the next best step in management. For example, in Canada the Canadian CT Head Injury/Trauma Rule allows physicians to safely rule out the presence of intracranial injuries that would require neurosurgical intervention without the need for CT imaging. It applies to patients with a Glasgow Coma Scale (GCS) of 13-15 and at least one of: Loss of consciousness, Amnesia to the head injury event, Witnessed disorientation. One can add points for high-risk criteria including: GCS <15 at 2 hours post-injury, suspected open or depressed skull fracture, signs of basilar skull fracture, 2 or more episodes of vomiting, age 65 or greater. Points are also given for medium risk criteria which include: retrograde amnesia of 30 minutes or more to the event, and dangerous mechanism (struck by motor vehicle, ejected from vehicle, fall from >3 feet or > 5 stairs [3]. Based on the score from tools such as the Canada CT Head Injury Rule, the next step typically involves either of observation, further imaging (I.e. urgent CT scans), or urgent surgical intervention. For the scenarios where further imaging is considered to be the next best step, the algorithm is typically as shown in Figure 1.

There are no universal standards for managing IH in spaceflight thus far; but it will require the development of unique space-specific decision-making tools. Some intracranial changes documented thus far in microgravity include augmented aqueductal cerebrospinal fluid hydrodynamics, and expansion of summated brain and cerebrospinal fluid volumes [4]. There remain many unanswered questions for the

physiology of IH in space. For-example it may be difficult to predict where blood pooling will occur following haemorrhages due to fluid shifts, or microgravity.

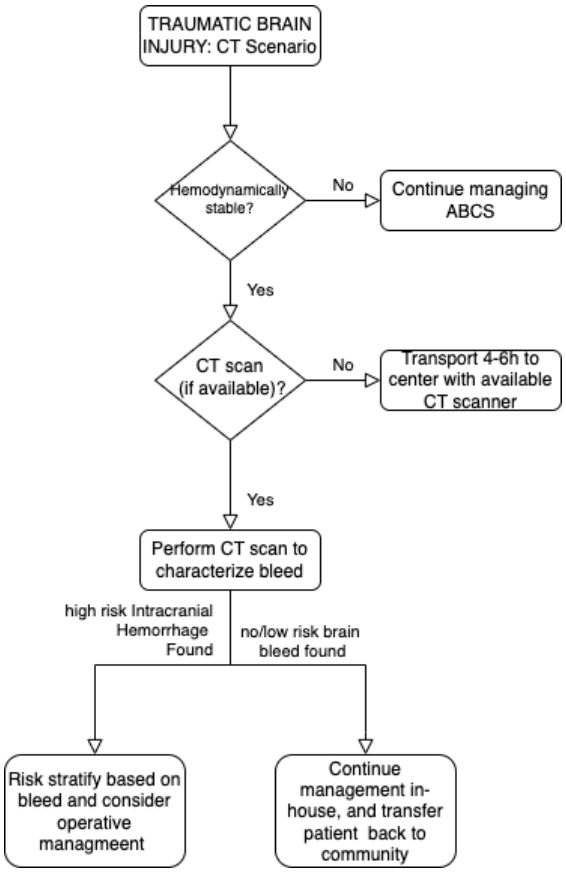

Figure 1: Algorithm for management of brain bleeds that necessitate further imaging.

1.3 Literature review of currently used alternative devices and technologies

Devices monitoring for intracranial hemorrhages vary in parameters such as accuracy, precision, cost, and operator dependence, thus their clinical utility can vary based on their user case. The BrainScope (Brainscope Company Inc., Bethesda, MD) device utilizes electroencephalography (EEG). EEG has been validated on board the ISS as part of the European Space Agency's NEUROSPAT investigation [5]. However, although EEG, may assist in identifying the latent effects of head trauma, it doesn't provide immediate diagnostic information to make timely management decisions for those experiencing traumatic head injuries.

Another method, laser speckle contrast imaging has been used to measure cerebral blood flow [6]. However, it is not suited for the application of detecting perimeningeal bleeds following head trauma as the technique does not penetrate well beneath the skull.

Phase Contrast CSF Flow MRI is a technique to assess the flow velocity of CSF; however, it is usually used to assess stroke volume in different brain regions following hemorrhage. One study established a strong link between hydrocephalus induced by subarachnoid hemorrhage and changes in CSF hydrodynamics [7]. It is therefore not a direct measurement of changes in the composition of the CSF which would indicate a bleed. Similarly, near-infrared transillumination backscattering sounding (NIR-T/BSS) has been used to measure changes in subarachnoid width due to systolic pulse waves [8], but information on the presence of blood is not provided.

Near-infrared (NIR) spectroscopy has now become a well-established method to detect changes in light absorbance below the skin. As far back as 1993, studies have looked into near infrared spectroscopy as a tool for localizing intracranial hematomas. Some studies suggested the technology could be useful as an adjunct to CT scanners [9]. Since then, the technology readiness level of NIR spectroscopy for the purposes of detecting intracranial hemorrhages has improved. For example, the InfraScanner 2000 (InfraScan, Inc., Philadelphia, PA), a portable NIR device has been developed and has shown that simulated hematomas larger than 3.5 cc and less than 2.5 cm from the surface of tissue phantoms can be detected with a sensitivity of 88% (95% confidence interval (CI) 74.9,95.0%), and specificity of 90.7% (95% CI 86.4,93.7%) [10].

In addition to facilitating excluding acute intracranial bleeding after minor head injury in adult populations, new studies suggest NIR can be used in paediatric populations – an example population where excessive use of CT scans are not favored due to radiation exposure [11]. Another study used the InfraScan NIRS device on board a helicopter medical response team and scoring the scan time, ease-of-use, and change in treatment. They found promising results using the InfraScan NIRS device in the prehospital screening for intracranial hematomas in TBI patients with high sensitivity and good specificity. However they felt that research would be necessary to determine the beneficial effects of enhanced prehospital screening on triage, survival, and quality of life in TBI patients [12]. We think that the triage and thus survival of TBI patients can be further improved if NIRS technology is adapted not just for detection but also quantification and analysis of brain bleeds. Specifically, we hypothesise that use of diffuse correlation spectroscopy can enable us to better characterize intracranial hemorrhages in the perimeningeal space.

1.4 Diffusion correlation spectroscopy

The primary challenge associated with deep tissue imaging is the absorption of the energy by water molecules. This causes significant attenuation of the

signal beyond a few millimeters into living tissues. This can be overcome by selecting a longer wavelength between the far- and near-infrared (NIR) region. Such wavelengths reside at the boundary of the THz frequency band (10^{12} Hz), which generally encompasses a spectrum between 0.3 THz – 30 THz. NIR waves possess much higher tissue penetration and generally present a low risk for operators and patients [13].

Despite NIR radiation's optimal penetrating depth, the highly scattering nature of biological tissues remains a significant challenge preventing any useful imaging resolution from being obtained. Human skull thickness varies between 3 – 9 mm depending on the region of the skull, age, sex, and other factors [14], which influences the path of emitted photons. Additionally, intracranial tissues have inhomogeneous NIR absorption and scattering which complicates our understanding of tissue properties at specific regions, such as the subarachnoid space.

THz radiation in the lower NIR range is particularly useful when applied to diffuse correlation spectroscopy, which is a technique that provides information about the velocity of scattering particles such as red blood cells (RBCs). It is a well-established technique [15] used commonly to measure cerebral blood flow; however, to date, the method is non-specific and usually averages the relative blood flow index (rBFI) according to the combined velocities of scattering particles in arteries (fast particles), capillaries (slow particles), as well as the general pulsatile systolic motion of all the interconnected tissues and fluids of the brain (stationary particles).

3. Theory and calculation

Figure 2 depicts a simplified model of these three types of scattering events (fast, slow, and static), with the static component represented by scattering in the tissue of the arachnoid mater, the slow component represented by scattering of a free particle suspended in the cerebrospinal fluid (CSF) of the subarachnoid space, and the fast component represented by scattering of RBCs traveling at high velocities inside blood vessels. We hypothesized that, by building upon existing models of cerebral blood flow, we could obtain the average particle velocity at specific tissue depths corresponding to the meningeal layers and isolate the specific velocity within the CSF. At the core of these existing models are the autocorrelation functions that correlate the rate of decay between the time-of-flight (TOF) of an imaginary photon reflected by an immobile object and TOF of the real photon which was reflected by a moving object. Importantly, it has been established that slow components of the amplitude do not fit models of intravascular forward scattering [16], thus providing evidence that these scatterers are extravascular and are mainly undergoing diffusive or Brownian motion. CSF in the subarachnoid space undergoes pulsatile bulk flow due to systolic pulse waves from nearby blood vessels (Fig. 2) [8], [17] but does not typically contain a significant number of scattering particles. Hence, the contribution of pure CSF to the signal amplitude is negligible. The rheological behaviour of normal CSF approximates that of water, a viscous Newtonian fluid [18]. If there were significant concentrations of proteins and RBCs in the CSF due to hemorrhage, the viscosity of CSF would increase [19], which hinders the advection, diffusion, and Brownian motion of particles. Consequently, the velocity of RBCs in the CSF would correspond to slow scattering events, which would be measurably more frequent for CSF containing blood compared to pure CSF. If the blood in the CSF formed a gel-like network due to the presence of clot-forming fibrin polymers, this would further increase viscosity, thus reducing particle motion in the fluid even more [20]. Measuring the diffusion coefficient of the tissue can provide estimates of these velocities.

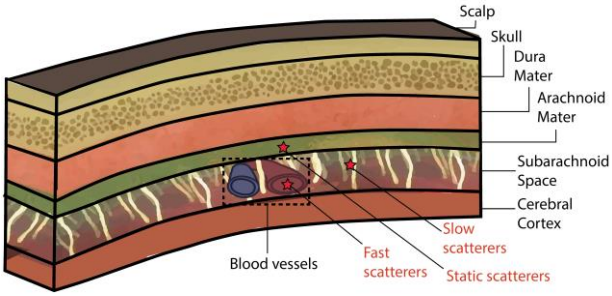

Figure 2. Diagram of simplified intracerebral layers with examples of static (components of the arachnoid mater), slow (Brownian motion of particles in the CSF of the subarachnoid space), and fast scattering particles (red blood cells within a blood vessel).

To measure the diffusion coefficient, we propose the use of a novel rBFI model established by Samaei et al. [21] previously validated with diffuse correlation spectroscopy. After getting the raw signal intensity of light scattered towards the detector of the NIR system, the data are fitted to an intensity autocorrelation function (Eq. 1), which is a summation of contributions from independent TOF-resolved decay rates. This enables the isolation of specific decay rates, corresponding to specific diffusion coefficients [21]:

$$g^{(M)}(t_s,\tau) = 1 + \beta \left| \sum_{m=1}^{M} a_m \exp\left[-\xi_m(t_s)\tau\right] \right|^2, \quad \sum_{m=1}^{M} a_m = 1 \tag{1}$$

One of the main confounding factors with this approach is the fact that decay rates inherently increase with tissue depth, since deeply penetrating photons undergo more scattering events than photons that

remain at shallow depths. Thus, what may be gated as a "slow decay rate" can be due to either faster dynamic scattering or deeper photon penetration. This is further compounded by the fact that each given tissue layer is inhomogeneous and contains fast and slow scatterers. This is exemplified by RBCs in tissues which have a velocity in arteries of 25 cm/s while in capillaries this decreases to about 0.2 cm/s. In general, it has been reported that the scalp and skull have slower autocorrelation decay rates compared to deeper cerebral layers [16]. One way to circumvent this problem is to apply pressure to the extracerebral layers which constricts superficial blood flow and reduces its contribution to the autocorrelation decay [21]. By doing this, one may be able to obtain a greater signal from the CSF in the subarachnoid space.

4. Results

4.1 Tissue phantom design

Many previous studies have utilized solid materials as tissue phantoms to validate brain hematomas due to the instability of liquid materials. However, since our theory depends on movement of particles driven by various forces such as Brownian motion, systolic pulses, and intravascular pumping in arteries, our validation studies must rely on phantoms that have both solid and liquid layers. CSF volume in the subarachnoid space is known to oscillate according to blood flow [8]. This can extend to the particles in the subarachnoid space which are expected to flow in oscillating directions, aligning with the flow of vascular blood [22]. By adjusting the viscosity of the liquid layers and adding channels through which pumped fluid represents vascular blood flow, we can mimic this pulsatile action for the validation of our diffuse correlation spectroscopy models (Fig. 3).

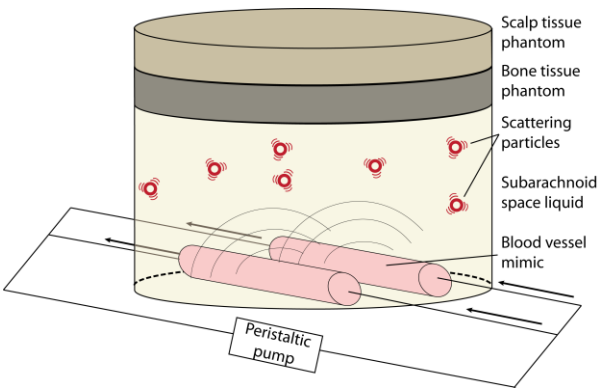

Figure 3. Sketch of a hybrid solid-liquid tissue phantom designed to study particle velocity.

The proposed components of the phantom along with their thicknesses are shown in Table 1. The scattering particles shown in Fig. 3 represent commercially available simulated blood used for ultrasound testing and training and bovine serum albumin (BSA), a small protein used to increase the viscosity of the CSF layer. The diffusion coefficient of BSA in phosphate buffered saline (PBS) at 37°C is 8.83x10-7 cm2/s [23] while the diffusion coefficient of hemoglobin inside RBCs is estimated at 1.1x10−7 cm2/s [24]. To approximate the scalp layer, standard polydimethylsiloxane (PDMS) will be used. The skull layer will be primarily composed of polyurethane (PU) because of its rigidity [25] and can be supplemented with titanium dioxide to increase its scattering coefficient and black pigment to increase its absorption coefficient [26].

Table 1. Proposed components for a hybrid solid-liquid phantom

Component	Material	Thickness (mm)
Scalp	PDMS	3
Skull	PU + TiO_2 + black pigment	5
Subarachnoid Space	PBS + simulated ultrasound blood + BSA	3
Blood Vessel	Reinforced hydrogel	1
Blood	Simulated ultrasound blood	—

To determine the minimum concentration of scattering particles (simulated blood and BSA) in the CSF layer needed for significant differences in the diffusion coefficient to be observed, we will test several iterations of our hybrid solid-liquid phantom. The CSF layer will be tested with various concentrations of simulated blood and BSA. The second iteration of the hybrid phantom will replace the BSA component with fibrin proteins, which are highly networked fibrillar proteins as opposed to the more globular nature of BSA. Fibrin is found in blood clots and would likely be found in CSF following IH. We also anticipate that fibrin will significantly impact the diffusion coefficient of nearby RBCs because of their fibrillar structure.

4.2 Hardware design

The imaging system envisioned for spaceflight will consist of a femtosecond pulsed laser at 855 nm that emits coherent NIR light from a handheld source-detector probe (Figure 4) attached by Velcro straps. The distance between the source and the detector was chosen as 10 mm, which is relatively small to capture more early to mid-TOF photons. This provides a greater resolution in the time delay between emission and detection. The measured amplitude and phase of the detected photons allows for the calculation of TOF and

intensity of the light, which is then processed to estimate tissue properties.

The operator will interact with the device by following the prompts on our user interface (UI) which will guide the operator through start-up, initiation, and measurements. The operator will place the probe as close to the skin as possible on the patient's head. Real-time fittings of the light's decay rates with the predicted "IH-positive" decay rates will be used to determine the likelihood of IH. Once a sufficient head area has been measured, the device's UI will provide the operator with the results.

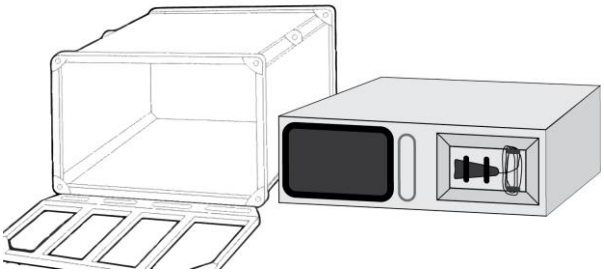

Figure 4. Basic sketch of the exterior of the imaging system (right) which includes a computer interface and the probe (attached via Velcro straps). A single international space station (ISS) middeck locker (left) is depicted to show the scale of the imaging system.

4.3 Operational constraints

To maximize the usefulness of our proposed technology not only for spaceflight but also for remote and rural clinical contexts, we have defined several design constraints for the hardware. The first constraint is related to the hardware's mass, volume, and power consumption. These specifications are important for space technologies where resources are limited. We have established that the maximum volume provided by the ISS double-width configuration of the Middeck Locker is an ideal benchmark. The volume should therefore not exceed 24.6" x 36.25" x 21.882" (inches).

Next, we have defined operational constraints for anticipated users of the device through consultations with primary care providers in rural health centers. In rural environments as well as in deep space, there is limited access to technicians for repair or maintenance of medical equipment, and there is limited infrastructure (it is common to experience unreliable phone service, internet, and electricity). Our proposed device must therefore be as self-contained as possible while requiring minimal external resources such as technicians and network connectivity. Next, there are many logistical challenges of transporting patients to medical facilities. For example, flights are infrequent and are often disrupted by weather, and ground transportation options can involve long bouts of travel on rugged gravel roads. To circumvent this problem, the hardware design should enable its implementation as close to the community as possible (e.g. community health clinics). The last operational constraint is related to the limited availability of medical personnel in remote environments. Primary care providers such as family physicians, nurse practitioners, and remote certified nurses are scarce and there is high staff turnover; therefore, the device should be easy to use and the data should be simple to interpret to enable non-medically trained personnel to operate it.

Finally, we also acknowledge that devices with multiple uses that can perform more than one task are better suited for resource-limited environments. Thus, versatility is a key element of the device's design. For example, the device could be adapted to image different parts of the body besides the head by adapting the source-detector probe.

4.4 Data management

Given the constraints listed above, the device will be designed to be fully autonomous, meaning that no data connection is required to use it. Astronauts on the ISS can therefore obtain full diagnostic information in real-time, which will ultimately improve patient outcomes since conditions involving head injuries are extremely time-sensitive. This is also particularly important for deep space (beyond low-Earth orbit) contexts where telecommunications with healthcare providers on Earth will have significant time delays. We will ensure that, even if the user has limited medical experience (which is a plausible scenario for deep space missions where a crew doctor may not be included), our device's user interface will minimize complexity of use and provide sufficient simple-to-interpret information. Regardless, we will also offer a framework that will enable the raw sensor data and/or derived information products to be quickly transmitted to an on-site patient/crew data management system as well as crew support personnel and healthcare providers off-site (e.g. flight surgeon on Earth) while adhering to patient-data privacy protocols.

When there is a scheduled or unexpected downtime between the users in a deep space mission, data that needs to be downlinked to off-site operations centers will be stored within the on-site data management system. When the network is back up online or intermittent, the highest priority patient data (either pre-configured or user-specified) will be downlinked first, followed by the next highest priority data defined by the downlink priority schemes.

4.5 Spaceflight feasibility study

To evaluate the feasibility and overall need for our proposed imaging system in space, we devised a scoring system with six criteria. Possible scores include "Yes", "No", and "Unknown" and are listed in Table 2.

Rationalizations and supporting evidence for each score are presented below.

Table 2. Evaluation of the need for a compact NIR imaging device for detection of IH during spaceflight

Criteria	Score
Does it fill a gap?	Yes
Does it significantly enhance med ops capabilities?	Unknown
Are there no alternatives?	Yes
Can it be implemented quickly (e.g. within the next 10 years)	Yes
Is it multi-purpose and/or does it have the potential to be useful for many applications?	No
Is there evidence to support its use?	Yes

Does it fill a gap? — For this criterion, we took into consideration the current capabilities on board the ISS to assess brain injuries. An EEG was used to assess changes in brain activity during spaceflight [27] but has never been used for IH. Because of the high resource cost of CT and MRI scanners, these are currently not available in space. In contrast, NIR spectroscopy is safe and portable, which could make it compatible with the constraints of spaceflight to fill an unmet gap.

Does it significantly enhance med ops capabilities? — This criterion was left open-ended until space analogue studies can provide further data to better understand the role of our proposed NIR spectroscopy device in the context of medical operations in space. We see potential challenges in obtaining sufficient specificity and sensitivity of the device to be widely accepted by crew doctors.

Are there no alternatives? — The alternative we have identified is to medevac the patient back to Earth to obtain a CT or MRI scan. This alternative quickly becomes unfeasible if we consider scenarios beyond low-Earth orbit.

Can it be implemented quickly (e.g. onto a spacecraft within the next 10 years) — Given that many of the hardware components already exist and given the relatively small resource footprint of the entire imaging system, we believe that there is strong evidence that it could be implemented onto the ISS before the station is decommissioned, which is currently planned for 2030.

Is it multi-purpose and/or does it have the potential to be useful for many applications? — This criterion is unfulfilled for the current iteration of the setup because its algorithms will solely be configured for detecting IH. In the future, it may be possible to extend the capabilities of the setup with minimal alterations to the hardware.

Is there evidence to support its use? — In this paper, we have provided comprehensive evidence that supports it as a useful tool for IH management in space.

5. Discussion

5.1 Considerations for operation due to microgravity and deep space radiation

Although the handheld probe should be simple to operate even in microgravity, there may still be concerns with keeping the patient immobilized. It is important that the probe remains stationary during measurements to obtain the best possible resolution and reduce artifacts. Thus, a stabilization mechanism such as an adjustable headpiece that connects the probe to the opposite side of the head is warranted for future design iterations.

Another complication potentially arising from the microgravity environment is the lack of information on the locations of blood pooling after a hemorrhage. On Earth, subarachnoid bleeds tend to pool predictably due to gravity but there is currently a lack of data on intracranial blood pooling in microgravity. Therefore, it is strongly suggested that future studies focus on this open area of research so that the resulting data may be used to improve brain imaging equipment used in space.

Cosmic background radiation in the deep space environment may also influence spectroscopy results. This has been observed as random, unidirectional peaks in Rahman spectroscopy data, and corrective algorithms have been developed to remove the noise [28], [29]. Similar corrections may also be applied to our proposed imaging system.

5.2 Potential applications beyond IH diagnosis

Most blood flow measurement techniques are tissue agnostic, meaning they can be used to measure the relative blood flow index in any tissue. Similarly, we anticipate that our proposed system could be used for other purposes beyond the diagnosis of IH. Because our method focuses on the measurement of diffusion coefficients to help identify changes in the motion of scattering particles in fluids found in deep tissues, it may be possible to scan for abnormal fluid build-up in other areas of the body. For example, pleural effusion is the build-up of fluid in the space between the chest wall and the lungs. The pleural fluid can contain different scattering components depending on the underlying cause [30], which may be detectable using our proposed technique with minor alterations to the probe stabilization mechanism.

5.3 Limitations

Red blood cells found in the intracranial spaces eventually undergo lysis and release hemoglobin, which is metabolized by local immune cells. This may cause significant changes in the way infrared light is scattered and the velocity of the scattering particles. Free hemoglobin has been shown to move at a higher velocity compared to hemoglobin inside whole red blood cells [24]. This signifies that measurements with

our proposed device need to be performed within a short period of time after trauma or the suspected cause of the hemorrhage, before lysis occurs. Otherwise, we may need to integrate an additional diffusion coefficient factor into the autocorrelation functions based on the length of time that has passed between the injury and the measurement.

Another limitation we have identified is that changes in CSF viscosity and subsequent changes in suspended particle diffusion rates could be due to other factors besides IH, which could contribute to false positive measurements. For example, meningitis is an inflammatory condition caused by bacteria in the meninges that leads to increased CSF viscosity [31]. To avoid such false positives, it is suggested to conduct a differential diagnosis to eliminate other causes of disease.

Lastly, the computational requirements for our system are very high. The complex functions governing the fitting for our autocorrelations require processing speeds only achievable with a desktop computer, which limits the portability of the system. This may be overcome by advances in processing power over time.

5.4 Planned validation studies

5.4.1 Static tissue baseline correction

Systolic pulse waves from the cardiovascular system generate small extensional motions of the tissues in proximity to vessels which need to be corrected to distinguish between static tissue structures and traveling scatterers such as RBCs inside blood vessels. Similar phase shift corrections have been used to generate more accurate autocorrelations for interferometric near-infrared spectroscopy [16]. Since our model will attempt to distinguish between the closely related velocities of static tissue and slow scatterers, it is even more important to accurately correct for bulk tissue motion.

5.4.2 Normalizing velocities to real-time blood pressure

Since our estimations of velocity of CSF scatterers in the subarachnoid space are directly dependent on the pressure exerted on CSF by vascular systolic pulse waves, we hypothesize that concurrent measurements of blood pressure (e.g. arm or finger cuff) could enable us to obtain greater accuracy. To fit a model of the relationship between blood pressure and diffusion coefficients of slow scattering events, we propose to use existing data from diffusion-weighted MRI measurements where patients also had their blood pressure monitored.

5.4.3 Estimating skull thickness

Due to bone's highly light-scattering nature, we have identified a need for an algorithm that can estimate skull thickness, which varies between individuals, from the data obtained from the reflected light. This will allow us to make adjustments to the cut-off between early TOFs and late TOFs (a measure of light penetration depth) and enable more accurate decay rates. To do this, we propose to run simulations in which we can modulate the skull thickness of the simulated tissue. In the future, CT images will be used to validate our methods during clinical trials. Therefore, we will have access to accurate skull thickness measurements from these CT images in order to validate the algorithms.

5.4.4 Machine learning training datasets

To train the software to produce an accurate prediction of IH, we will first use the data produced by our hybrid phantoms. By varying several features of the hybrid phantoms, we can create a diverse dataset needed for supervised machine-learning methods to segregate IH from non-IH.

Due to the inherent difficulty in collecting representative data from hybrid phantoms, and lack of public dataset resources, the volume, variety, and a veracity of our training data may be insufficient. Exploration into the use of generative adversarial networks (GANs) as a method of synthetic THz training data. Furthermore, efforts will be made to explore use of neural nets to replace various data processing steps in the signal extraction process.

6. Conclusions

In this work, we have presented a realistic concept for an NIR-based brain imaging technique that is suitable for the space environment. The system is based upon existing NIR spectroscopic capabilities with the addition of novel models to analyze the data and extract information about the diffusion coefficient of CSF in the subarachnoid space. It is important to distinguish that the system we propose here is not intended to replace the gold standard CT scanner. Rather, we envision this technology as a means to provide more information to an astronaut crew that must decide whether a suspected brain injury is severe enough to warrant emergency intervention, including confirmation by CT back on Earth. The decision to medevac an astronaut back to Earth amidst a mission has serious consequences and complications, not only for the completion of the mission but also for the health and safety of the crew. As such, despite the probable issues with specificity and sensitivity that such an NIR imaging system could have when compared to CT, we believe that it has tremendous potential for human spaceflight. Furthermore, there are applications for remote terrestrial environments as well, which usually have limited access to CT scanners and other state-of-the-art tools to diagnose IH.

Acknowledgements

We would like to acknowledge Dr. Jeffrey Beselt, MD, CCFP(EM), FCFP for his assistance in defining the operational constraints of our design.

References

[1] U. C. Schneider, R. Xu, and P. Vajkoczy, "Inflammatory Events Following Subarachnoid Hemorrhage (SAH)," *Curr. Neuropharmacol.*, vol. 16, no. 9, pp. 1385–1395, Nov. 2018, doi: 10.2174/1570159X16666180412110919.

[2] N. K. Joshi and Y. Okuda, "Intracranial Hemorrhage," *Simwars Simul. Case Book Emerg. Med.*, pp. 159–163, Feb. 2022, doi: 10.1017/CBO9781107111011.039.

[3] I. G. Stiell *et al.*, "A prospective cluster-randomized trial to implement the Canadian CT Head Rule in emergency departments," *CMAJ*, vol. 182, no. 14, pp. 1527–1532, Oct. 2010, doi: 10.1503/CMAJ.091974.

[4] L. A. Kramer *et al.*, "Intracranial effects of microgravity: A prospective longitudinal MRI study," *Radiology*, vol. 295, no. 3, pp. 640–648, Jun. 2020, doi: 10.1148/RADIOL.2020191413/ASSET/IMAGES/LARGE/RADIOL.2020191413.FIG6C.JPEG.

[5] M. F. Dinatolo and L. Y. Cohen, "Monitoring the Impact of Spaceflight on the Human Brain," *Life*, vol. 12, no. 7, Art. no. 7, Jul. 2022, doi: 10.3390/life12071060.

[6] A. K. Dunn, "Laser Speckle Contrast Imaging of Cerebral Blood Flow," *Ann. Biomed. Eng.*, vol. 40, no. 2, pp. 367–377, Feb. 2012, doi: 10.1007/s10439-011-0469-0.

[7] G. Saliou *et al.*, "A Phase-Contrast MRI Study of Acute and Chronic Hydrodynamic Alterations after Hydrocephalus Induced by Subarachnoid Hemorrhage," *J. Neuroimaging*, vol. 22, no. 4, pp. 343–350, 2012, doi: 10.1111/j.1552-6569.2011.00594.x.

[8] M. Gruszecki *et al.*, "Human subarachnoid space width oscillations in the resting state," *Sci. Rep.*, vol. 8, no. 1, Art. no. 1, Feb. 2018, doi: 10.1038/s41598-018-21038-0.

[9] S. P. Gopinath, C. S. Robertson, R. G. Grossman, and B. Chance, "Near-infrared spectroscopic localization of intracranial hematomas," *J. Neurosurg.*, vol. 79, no. 1, pp. 43–47, Jul. 1993, doi: 10.3171/JNS.1993.79.1.0043.

[10] C. S. Robertson *et al.*, "Clinical Evaluation of a Portable Near-Infrared Device for Detection of Traumatic Intracranial Hematomas," *J. Neurotrauma*, vol. 27, no. 9, pp. 1597–1604, Sep. 2010, doi: 10.1089/neu.2010.1340.

[11] D. Lewartowska-Nyga, K. Nyga, and G. zyna Skotnicka-Klonowicz, "Can infrascanner be useful in hospital emergency departments for diagnosing minor head injury in children?," *Dev. Period Med.*, vol. 21, no. 1, p. 51, Jan. 2017, doi: 10.34763/DEVPERIODMED.20172101.5159.

[12] J. Peters, B. Van Wageningen, N. Hoogerwerf, and E. Tan, "Near-infrared spectroscopy: a promising prehospital tool for management of traumatic brain injury," *Prehosp Disaster Med*, vol. 32, no. 4, pp. 414–418, Aug. 2017, doi: 10.1017/s1049023x17006367.

[13] A. Bozkurt and B. Onaral, "Safety assessment of near infrared light emitting diodes for diffuse optical measurements," *Biomed. Eng. OnLine*, vol. 3, no. 1, p. 9, Mar. 2004, doi: 10.1186/1475-925X-3-9.

[14] H. A. Mahinda and O. P. Murty, "Variability in Thickness of Human Skull Bones and Sternum – an Autopsy Experience," *J. Forensic Med.*, vol. 26, pp. 26–31, 2009.

[15] D. A. Boas and A. G. Yodh, "Spatially varying dynamical properties of turbid media probed with diffusing temporal light correlation," *JOSA A*, vol. 14, no. 1, pp. 192–215, Jan. 1997, doi: 10.1364/JOSAA.14.000192.

[16] O. Kholiqov, W. Zhou, T. Zhang, V. N. Du Le, and V. J. Srinivasan, "Time-of-flight resolved light field fluctuations reveal deep human tissue physiology," *Nat. Commun.*, vol. 11, no. 1, Art. no. 1, Jan. 2020, doi: 10.1038/s41467-019-14228-5.

[17] L. Sakka, G. Coll, and J. Chazal, "Anatomy and physiology of cerebrospinal fluid," *Eur. Ann. Otorhinolaryngol. Head Neck Dis.*, vol. 128, no. 6, pp. 309–316, Dec. 2011, doi: 10.1016/j.anorl.2011.03.002.

[18] I. G. Bloomfield, I. H. Johnston, and L. E. Bilston, "Effects of Proteins, Blood Cells and Glucose on the Viscosity of Cerebrospinal Fluid," *Pediatr. Neurosurg.*, vol. 28, no. 5, pp. 246–251, 1998, doi: 10.1159/000028659.

[19] R. E. Klabunde and Lippincott Williams & Wilkins., *Cardiovascular Physiology Concepts*, 3rd ed. Wolters Kluwer Health, 2020. [Online]. Available: http://whel-primo.hosted.exlibrisgroup.com/openurl/44WHELF_NLW/44WHELF_NLW_services_page?u.ignore_date_coverage=true&rft.mms_id=991090043202419

[20] M. Ranucci, T. Laddomada, M. Ranucci, and E. Baryshnikova, "Blood viscosity during coagulation at different shear rates," *Physiol. Rep.*, vol. 2, no. 7, p. e12065, Jul. 2014, doi: 10.14814/phy2.12065.

[21] S. Samaei, P. Sawosz, M. Kacprzak, Ż. Pastuszak, D. Borycki, and A. Liebert, "Time-domain diffuse correlation spectroscopy (TD-DCS) for noninvasive, depth-dependent blood flow quantification in human tissue in vivo," *Sci. Rep.*, vol. 11, no. 1, Art. no. 1, Jan. 2021, doi: 10.1038/s41598-021-81448-5.

[22] J. H. Thomas, "Fluid dynamics of cerebrospinal fluid flow in perivascular spaces," *J. R. Soc. Interface*, vol. 16, no. 159, p. 20190572, Oct. 2019, doi: 10.1098/rsif.2019.0572.

[23] A. K. Gaigalas, J. B. Hubbard, M. McCurley, and S. Woo, "Diffusion of bovine serum albumin in aqueous solutions," *J. Phys. Chem.*, vol. 96, no. 5, pp. 2355–2359, Mar. 1992, doi: 10.1021/j100184a063.

[24] W. Doster and S. Longeville, "Microscopic Diffusion and Hydrodynamic Interactions of Hemoglobin in Red Blood Cells," *Biophys. J.*, vol. 93, no. 4, pp. 1360–1368, Aug. 2007, doi: 10.1529/biophysj.106.097956.

[25] T. P. Moffitt, Y.-C. Chen, and S. A. Prahl, "Preparation and characterization of polyurethane optical phantoms," *J. Biomed. Opt.*, vol. 11, no. 4, p. 041103, Jul. 2006, doi: 10.1117/1.2240972.

[26] J. Wang, J. Lin, Y. Chen, C. G. Welle, and T. J. Pfefer, "Phantom-based evaluation of near-infrared intracranial hematoma detector performance," *J. Biomed. Opt.*, vol. 24, no. 4, p. 045001, Apr. 2019, doi: 10.1117/1.JBO.24.4.045001.

[27] G. Petit *et al.*, "Local sleep-like events during wakefulness and their relationship to decreased alertness in astronauts on ISS," *Npj Microgravity*, vol. 5, no. 1, Art. no. 1, May 2019, doi: 10.1038/s41526-019-0069-0.

[28] S. J. Barton and B. M. Hennelly, "An Algorithm for the Removal of Cosmic Ray Artifacts in Spectral Data Sets," *Appl. Spectrosc.*, vol. 73, no. 8, pp. 893–901, Aug. 2019, doi: 10.1177/0003702819839098.

[29] C. J. F. Bertens *et al.*, "Pipeline for the removal of hardware related artifacts and background noise for Raman spectroscopy," *MethodsX*, vol. 7, p. 100883, Jan. 2020, doi: 10.1016/j.mex.2020.100883.

[30] S. A. Sahn, "Getting the most from pleural fluid analysis," *Respirology*, vol. 17, no. 2, pp. 270–277, 2012, doi: 10.1111/j.1440-1843.2011.02100.x.

[31] F. Yetkin, U. Kayabas, Y. Ersoy, Y. Bayindir, S. A. Toplu, and I. Tek, "Cerebrospinal fluid viscosity: a novel diagnostic measure for acute meningitis," *South. Med. J.*, vol. 103, no. 9, pp. 892–895, Sep. 2010, doi: 10.1097/smj.0b013e3181ebe260.